

PVP2018-84352

## THE FLUID ELASTIC INSTABILITY OF CONCENTRIC ARRAYS OF TUBE BUNDLES SUBJECTED ON CROSS FLOW

**Liyan Liu**

School of Chemical Engineering  
and Technology of Tianjin  
University  
Tianjin, China

**Wei Xu**

School of Chemical Engineering  
and Technology of Tianjin  
University  
Tianjin, China

**Kai Guo**

School of Chemical Engineering  
and Technology of Tianjin  
University  
Tianjin, China

**Zhanbin Jia**

School of Chemical Engineering  
and Technology of Tianjin  
University  
Tianjin, China

**Yang Wang**

School of Chemical Engineering  
and Technology of Tianjin  
University  
Tianjin, China

**Wei Tan**

School of Chemical Engineering  
and Technology of Tianjin  
University  
Tianjin, China

### ABSTRACT

Concentric arrays of tube bundles are applied extensively in heat exchangers at nuclear power plants. Flow induced vibration is one of the main causes of heat exchanger failures. However, there is no corresponding standard and basic parameters in the design code of different countries for concentric arrays of tube bundles. The fluid elastic instability of this type of heat exchangers cannot be calculated, and the design criteria is lacked. In this paper, a circulating water tunnel experimental facility were set up to test the vibration characteristic of concentric arrays subjected to cross flow. A non-contact measurement method based on high-speed photography imaging technology were adopted, which improved the accuracy of the test. Three kinds of tube bundles (0-degree angle, 15-degree angle and 30-degree angle arrangement, radial/circumferential pitch being 33.6/36.4 mm) were studied. The vibration frequency, amplitude and critical velocity of the tube bundle were investigated by changing the flow velocity. Computational fluid dynamics and fluid-structure interaction method were applied to simulate the fluid elastic instability of tube bundles, that were further verified by the experiments. Meanwhile, the numerical simulation supplements the contents of the experimental studies, which is utilizable to investigate and research the fluid elastic instability. The results of this work could provide references for the design of concentric array heat exchangers.

### KEY WORDS

Fluid elastic instability; Concentric arrays; High-speed photograph imaging technology; fluid-structure interaction; Critical velocity

### INTRODUCTION

Concentric tube arrays are widely adopted in heat exchangers in nuclear industry. Safety is more important for radioactive nuclear components, which should be given sufficient attention. Flow induced vibration (FIV) often occurs in heat exchanger tubes bundles subjected to cross flow. Base on the research of Pettigrew et al [1] and Gorman [2], the mechanisms of FIV include periodic vortex shedding, random excitation due to turbulence and fluid elastic instability (FEI), among which FEI is the most common and destructive mechanism. FEI is the result of a dynamic fluid force interacting with the motion of a tube. Once the flow velocity reaches critical value, it causes a substantial vibration and leads to rapid wear of the tube at the support.

In order to predict the FEI of heat exchanger tube bundles, many scholars put forward different mathematical models, which can be expressed in a unified formula [3, 4]

$$[M_s + M_f] \{\ddot{Q}\} + [C_s + C_f] \{\dot{Q}\} + [K_s + K_f] \{Q\} = \{G\} \quad (1)$$

where  $\{\ddot{Q}\}$ ,  $\{\dot{Q}\}$  and  $\{Q\}$  are the acceleration, velocity and displacement of the structure, respectively;  $[M_s]$  and  $[M_f]$  are the structural and additional mass, respectively;  $[C_s]$  and  $[C_f]$  are structural and fluid damping, respectively;  $[K_s]$  and  $[K_f]$  are structural and fluid stiffness, respectively;  $\{G\}$  is external exciting force. Existing mathematical models can be mainly grouped into three categories, quasi-static model [5, 6], quasi-steady model [7, 8] and unsteady model [9, 10 and 11]. There are also jet switch model proposed by Roberts [12], semi-analytical model proposed by Lever and Weaver [13].

When the tube bundle is excited by FEI, it is common to use the semi-empirical formula first proposed by Connors [5] to calculate the critical velocity from a practical point of view,

$$\frac{v_c}{fd} = K \left( \frac{m\delta}{\rho d^2} \right)^{\frac{1}{2}} \quad (2)$$

where  $v_c$  is critical velocity (m/s);  $m$  is the mass of unit length tube, including the additional mass of the fluid (kg/m);  $\rho$  is the density of the fluid outside the tube (kg/m<sup>3</sup>);  $f$  is the natural frequency of tube (Hz);  $\delta$  is logarithmic decay rate of tube;  $K$  is experience coefficient.

The earliest recorded systematic experiments on FEI was from Grover and Weaver [14]. A set of tube bundle containing 19 tubes was used in the experiment. One of the tubes was a flexible tube and the other were rigid. The similarities between the instability of single tube and that of the whole tube bundle were summarized through experiment. Tanaka et al [15] experimentally determined the unsteady fluid force applied to the tube bundle at various pitch-to-diameter ratios. Critical velocity characteristics of tube bundles with different pitch-to-diameter ratios were discussed after analyzing the results. Based on the unsteady theory, Chen et al [16] proposed a number of fluid elastic force coefficients and added the force to the system as excitation source. The mechanical equation was similar to the linear expression established by Tanaka. The conclusion was drawn that the fluid elastic coefficient was related to the bundle array, pitch-to-diameter ratio, amplitude, critical velocity and Reynolds number. Prakash et al [17] studied the FIV measurements carried out in 60-degree angle sector model of concentric array tube bundles. Although a large number of theoretical and experimental studies have been conducted on FIV since 1960s, there is not a criterion that can ubiquitously and accurately predict the FEI of the tube bundle in all cases, among which there are few studies on concentric arrays of tube bundles.

The visual image processing system has potential application for vibration analysis [18], which was first proposed in the 1980s [19, 20]. With the development of computer technology and image acquisition technology, this method has been widely applied in recent years. The basis of this method is that the surface of the testing object is coated with a pigment that is clearly distinguishable from the background, making it easy to be identified [21, 22]. This is a

non-contact test method. Compared with the contact test method, it is easy to monitor multiple tubes simultaneously, with high accuracy and low cost, and also there will be no test components interfering with the flow field.

With the rise of computational fluid dynamics (CFD) in recent years, numerical methods are widely applied in the study of FIV. Large eddy simulation (LES) technique is a direct calculation of large vortex scale, while small vortex scale is approximated. Hassan et al [23-26] first used two-dimensional LES model to study the flow around the tube. Omar [27] applied commercial CFD simulation software ANSYS CFX to study the FEI of flexible tube bundle in two-dimensional scale. The results were compared with the previous experiment, which were in good agreement. A lot of research has been done on the flow around the tube bundle, but still lack of numerical studies of the tube bundle vibration. As the FIV of the tube bundles usually involves complex phenomena of fluid-structure interaction, the numerical realization is a bit difficult and the numerical study in this area still needs further study.

In the existing heat exchanger standards and design codes, only several of the most common arrays of tube bundles are specified. With the development of nuclear power, more and more special arrays of tube bundles are utilized, including concentric array. In order to study FEI of concentric arrays of tube bundles, a set of visualized vibration measurement system was adopted, and a comparative study was carried out by using CFD. This work lays emphasis on the critical velocity, vibration frequency, amplitude, the main vibration direction and other FEI characteristics, in the hope of providing guidance on the design and operation of this kind of heat exchangers.

## NOMENCLATURE

FIV	Flow induced vibration
FEI	Fluid elastic instability
$M$	Mass matrix
$Q, \dot{Q}, \ddot{Q}$	Structure displacement, velocity and acceleration
$C$	Damping matrix
$K$	Stiffness matrix
$v_c$	Critical velocity
$\rho$	Fluid density
$f$	Tube natural frequency
$\delta$	Tube logarithmic decay rate
CFD	Computational fluid dynamics
LES	Large eddy simulation
$F$	Composition of forces on the tube
$k_{spring}$	Stiffness coefficient of spring
$U_g$	Mean gap velocity

## SUBSCRIPT

$f$	Fluid
$s$	Structure

## EXPERIMENTAL SETUP

In order to measure the vibration of tube bundles, a visual vibration measurement system, shown in Fig. 1, based on high-speed photography imaging technology, was designed, consisting of a test tube bundle, a water tunnel test system, a visual image processing system and a data processing system.

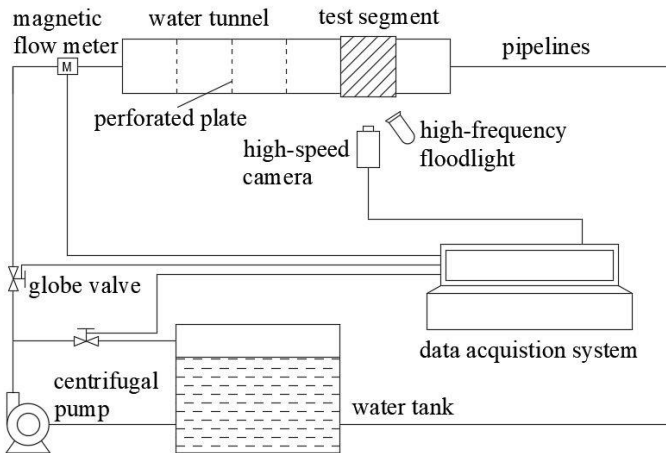


Fig. 1 Schematic of the visual vibration measurement system

## Test tube bundles

In this paper, the concentric arrays of tube bundles were studied. The fluid normally flows into the tube bundle from all directions in this arrangement. It has a rotational periodicity, which takes 60-degree angle as a cycle. Three representative incident angles can be selected, 0-degree angle, 15-degree angle and 30-degree angle, respectively, as shown in Fig. 2. The tube pitch is same for all three locations (radial/circumferential pitch being 33.6/36.4 mm).

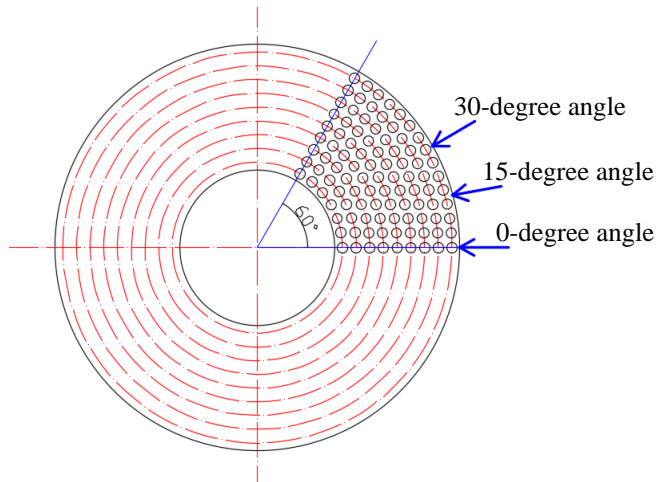


Fig. 2 Tube bundles

There are two kinds of tubes, flexible tubes and rigid tubes, as shown in Fig. 3. Flexible tubes are made of aluminum alloy and rigid tubes are made of steel. Both of them have similar surface roughness to real heat exchanger tubes. Flexible tubes consist of thick parts (250 mm) and thin parts (100 mm).

The diameter of test section of cylinders is 25 mm. All tubes are threaded into the replaceable tube plate.

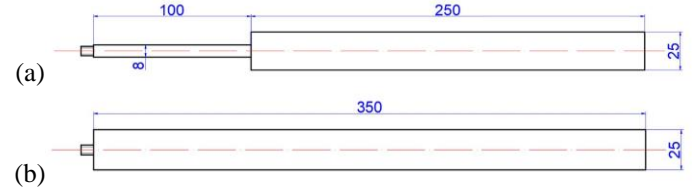


Fig. 3 Tube specimens. (a) flexible tube; (b) rigid tube

The tube bundle consists of flexible tubes in the center region and surrounding rigid tubes. The natural frequency of rigid tube is 140.6Hz, which is far greater than that of flexible tube. Therefore, in this experiment, rigid tubes are considered to be stationary.

## Water tunnel test system

Water tunnel test system includes a horizontal water tunnel, a test section, a flowmeter, a centrifugal pump, a water tanks, perforated plates, pipelines and valves. Perforated plates are set to obtain uniformly distributed inflow. The flow is changed by adjusting the opening of valves.

The length of the test section is 500 mm with a rectangular cross section. Cross-sectional schematic is shown in Fig. 4. Tubes are placed horizontally in order to facilitate the vibration test. The effect of gravity on the tubes is small and negligible. The turbulence intensity of the fluid is very low (<5%) through the steady-flow zone in the upstream of the test section.

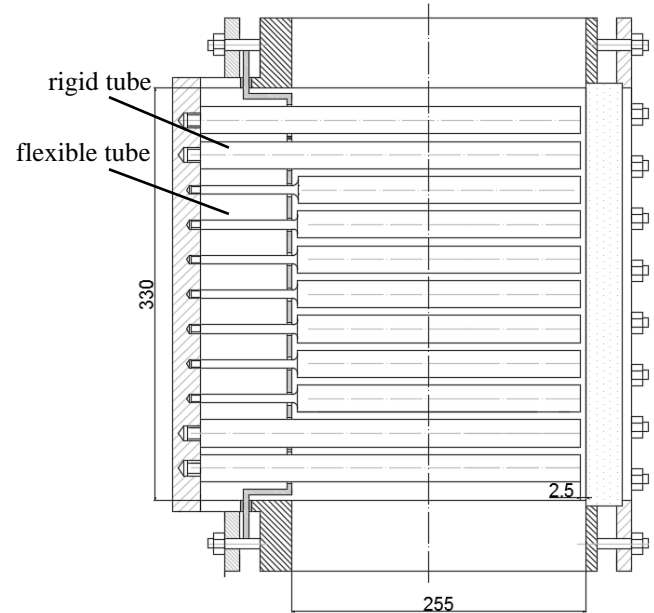


Fig. 4 Cross-sectional schematic of test section

## Visual image processing system and data processing system

Visual image processing system is adopted, as shown in Fig. 5. High-speed camera sampling frequency is set to 400 FPS and the movement of the tubes can be clearly recorded at

this frame rate. A high-frequency floodlight provides sufficient brightness to make the image contour clear. The ends of the tubes are painted white for easier identification. Electric power source can provide high-frequency AC, which is much higher than sampling frequency, to improve image qualities. A self-developed software is used to process the motion images of tubes.

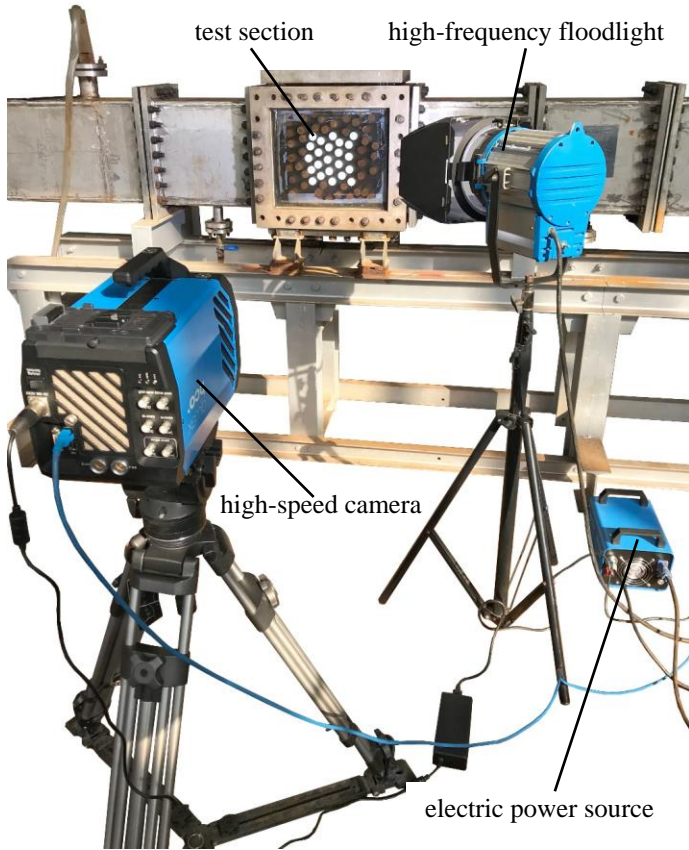


Fig. 5 Visual image processing system

The principle of the analysis software is to identify tubes and record the movement of tubes. The images captured by high-speed camera are converted to black-and-white mode. The flexible tubes are clearly separated from the background by adjusting the brightness and contrast. Then the boundaries and centroids of tubes are recognized. Envelope circles based on the boundaries of tubes are also generated. The centroids of the boundaries and the centers of the envelope are compared. If the difference between the two is within the acceptable error range, the recognition is considered as accurate, as shown in Fig. 6. Then motion coordinate information in the time domain are outputted as text documents.

### Experimental design

#### *Experiments design in air*

In order to obtain the natural frequency of the flexible tube and to compare the visual vibration measurement method with the traditional strain test method, a free attenuation vibration test in the air was required. Visual vibration measurement

method analyzes from the perspective of displacement, while traditional strain test method analyzes from the point of force. Therefore, it was necessary to convert the strain data to the displacement of the tube end face. Strain gauges are set on the thin part of flexible test tube in advance. When the device was installed, the free end of the tube was knocked to make the tube free attenuation vibrate. Both methods were tested at the same time. Sampling time should be longer than 10 seconds to ensure the accuracy of the result.

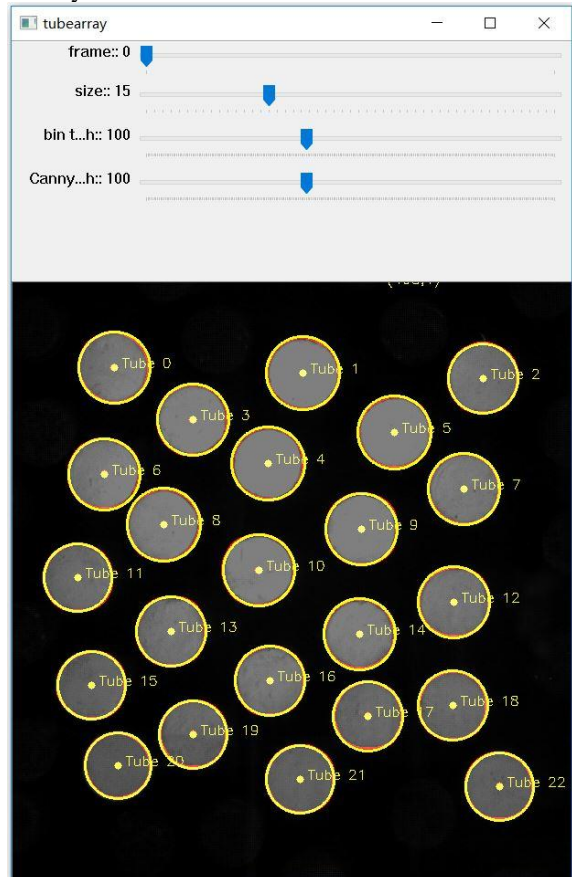


Fig. 6 Data processing system

#### *Experiments design in water*

The establishment of full-size tube bundle model will undoubtedly greatly increase the manufacturing and test workload. For the purpose of conducting a comprehensive study on the characteristics of FEI of concentric arrays of tube bundles and reducing the workload at the same time, three representative locations were selected for local experimental study, and named according to the inflow angle, which were 0-degree angle, 15-degree angle and 30-degree angle arrangement.

The 0-degree angle arrangement contained 25 flexible tubes, while the 15-degree angle arrangement and 30-degree angle arrangement contained 22 and 23 flexible tubes, respectively. Rigid tubes were placed around the flexible tubes to simulate the real heat exchanger flow field environment and minimize end-effects of the test section walls. Flexible and

rigid tubes distributions are shown in Fig. 7. For each arrangement, a flexible tube at the center was selected as the key item, which was identified as tube C.

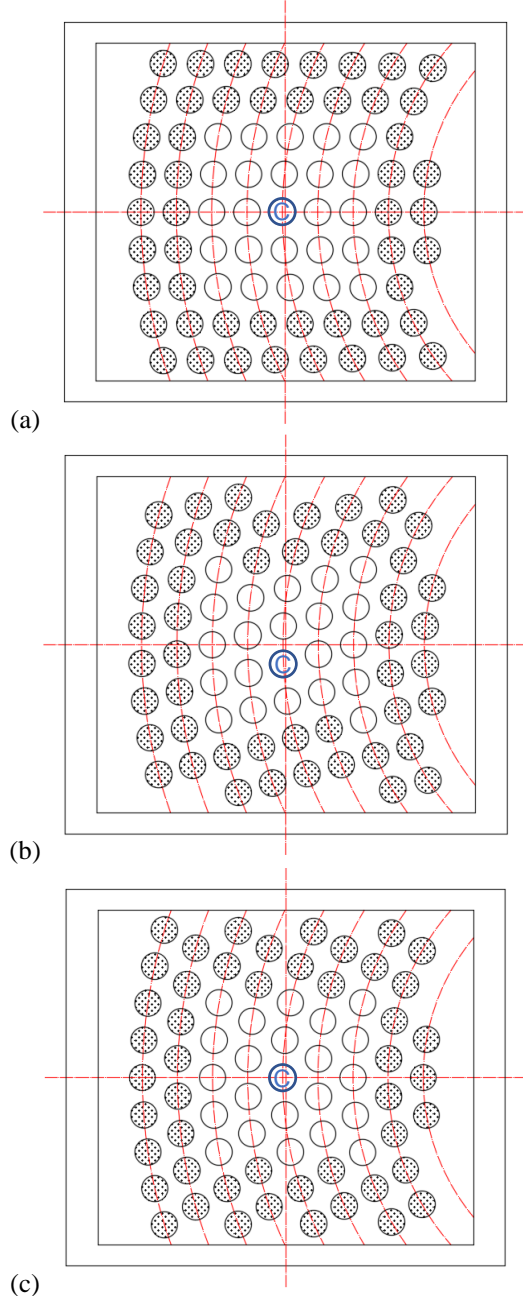


Fig. 7 Flexible and rigid tubes distribution. (a) 0-degree angle; (b) 15-degree angle; (c) 30-degree angle

After installing the tube bundle, the motion characteristics of tubes under different inflow velocities (0~0.97 m/s) could be obtained by adjusting the water channel flow (0~300 m<sup>3</sup>/h), while Reynolds numbers varied from 0 to 3×10<sup>5</sup>. After each adjustment of the flow rate, wait for the flow rate to stabilize and start sampling. To ensure adequate data, the sampling time should be at least 10 seconds. Through the experimental data

analysis, the main vibration direction, vibration amplitude, critical velocity, vibration frequency and other parameters were analyzed.

## NUMERICAL SIMULATION SETUP

The numerical simulation models of FEI of concentric tubes for heat exchange tube bundle was established by using commercial numerical simulation software ANSYS CFX. The simulation study on FEI was carried out compared with the experimental results.

### Fluid-structure interaction model of tube bundles

FEI involves the bidirectional interaction of fluid and solid domains, and large-scale numerical simulations are still difficult to achieve. A simplified fluid-structure interaction model was established through the use of rigid body structure and dynamic mesh technology.

Actual heat exchanger tube is very long. The large size of model will lead to too many meshes, which is difficult to calculate. Therefore, periodic boundary conditions were used to simplify the model. Quasi two-dimensional model was established that only a layer of meshes was generated, and the symmetric plane was set.

The rigid body structure was adopted to simplify the model, indicating that tubes were considered as non-deformable rigid bodies and spring restrains were applied at both ends of tubes, as shown in Fig. 8. This kind of model is widely used in the study of FEI of heat exchanger tube bundles.

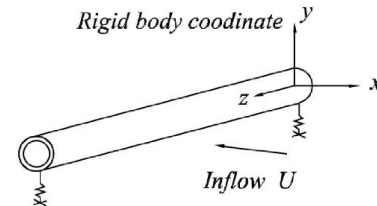


Fig. 8 Rigid body cylinder vibration system

The motion equation of the rigid body can be expressed as

$$m\ddot{Q} = F = F_D - k_{spring}(Q - Q_0) + F_{Ext} \quad (3)$$

where  $F$  is composition of forces on the tube (N);  $F_D$  is fluid force on the tube (N);  $F_{Ext}$  is extra force on the tube (N);  $k_{spring}$  is stiffness coefficient of spring (N/m);  $Q$ ,  $Q_0$  are displacement and initial displacement of the tube (m). Bundle stiffness could be entered directly in rigid body of calculated boundary. For damping force, tube velocity was extracted from each iteration firstly and then multiplied by the damping. Damping force in the form of extra force was fed back to iterative computing.

### Model geometry and boundary conditions setup

Corresponding to the experiment, numerical simulation models are shown in Fig. 9. The flexible tubes were correspondingly set as rigid body motion boundaries and as independent coordinate systems. The LES turbulence model was used to calculate the free vibration of the tube bundle

under the action of fluid force. Sampling time was 5 seconds. The calculation setup and boundary conditions are shown in Table 1.

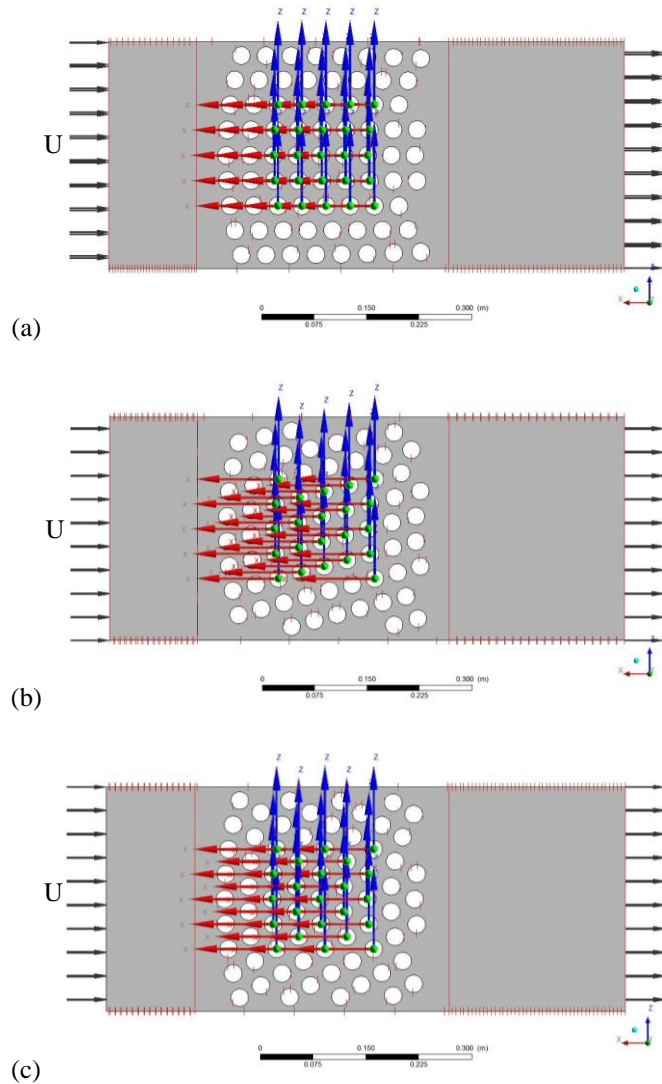


Fig. 9 Numerical simulation models. (a) 0-degree angle; (b) 15-degree angle; (c) 30-degree angle

Table 1 Calculation setup and boundary conditions

Items	Setup
analysis type	transient analysis
fluid medium	water
turbulence model	LES WALE
inlet condition	even flow
outlet condition	pressure outlet
symmetry surface condition	periodic boundary condition
tube wall condition	rigid body wall, dynamic mesh
wall function	scalable wall function

## RESULT AND DISCUSSION

### Free attenuation vibration

The purpose of free attenuation vibration test in the air is to verify the accuracy of the visual image processing system, get the logarithmic decay rate and other key parameters by acquiring the natural frequency. The results were averaged from three tests to reduce errors and the two methods were compared in Table 2. It can be seen that the results of natural frequency are very similar with a difference of 0.16 Hz. Visual vibration measurement method can be considered accurate, which will be adopted in later experiments.

Table 2 Result of free attenuation vibration test in the air

Visual vibration measurement method /Hz	Traditional strain test method /Hz	Relative error /%
19.19	19.03	0.8

### Critical flow velocity

The critical flow velocity is an important indicator of FEI. In the tube bundle, when the fluid flow velocity reaches the critical flow velocity, the tube will vibrate violently under the mechanism of FEI. Therefore, the sharp increase of root mean square (RMS) amplitude is an important criterion for judging FEI. However, it is also considered as the appearance of FEI when RMS amplitude reaches 2% of the tube diameter (0.5 mm) if not with a sharp increase. During experiments, the whole process of vibration could be observed through visual inspection method. When the velocity increased to a certain extent, significant vibration occurred in the tube bundle, showing that FEI occurred.

In the analysis of the tube bundle system, mean gap velocity,  $U_g$ , is commonly used to characterize the flow velocity in the tube bundle. Trial and CFD methods were applied respectively to obtain displacement responses of three kinds of arrangements. RMS amplitudes at different mean gap velocities were obtained as shown in Fig. 10.

The critical flow velocities of different arrangements are different, as listed in Table 3. It could be seen that the CFD results are the same as the experimental results on the overall trend of change, which verifies the feasibility of CFD method. However, the results obtained by the two methods are a bit different for two main reasons. Firstly, in order to reduce the calculation scale, the actual three-dimensional models were simplified to two-dimensional models, resulting in a certain impact on the accuracy of the calculation. Secondly, the tubes were in an ideal and uniform state in CFD, while there were inevitably some deviations in the actual manufacturing and installation of experimental equipment, which affected the experiment results. In general, the CFD method of fluid-structure interaction used in this paper could be applied to study the FEI of tube bundle vibration even with minor deviation.

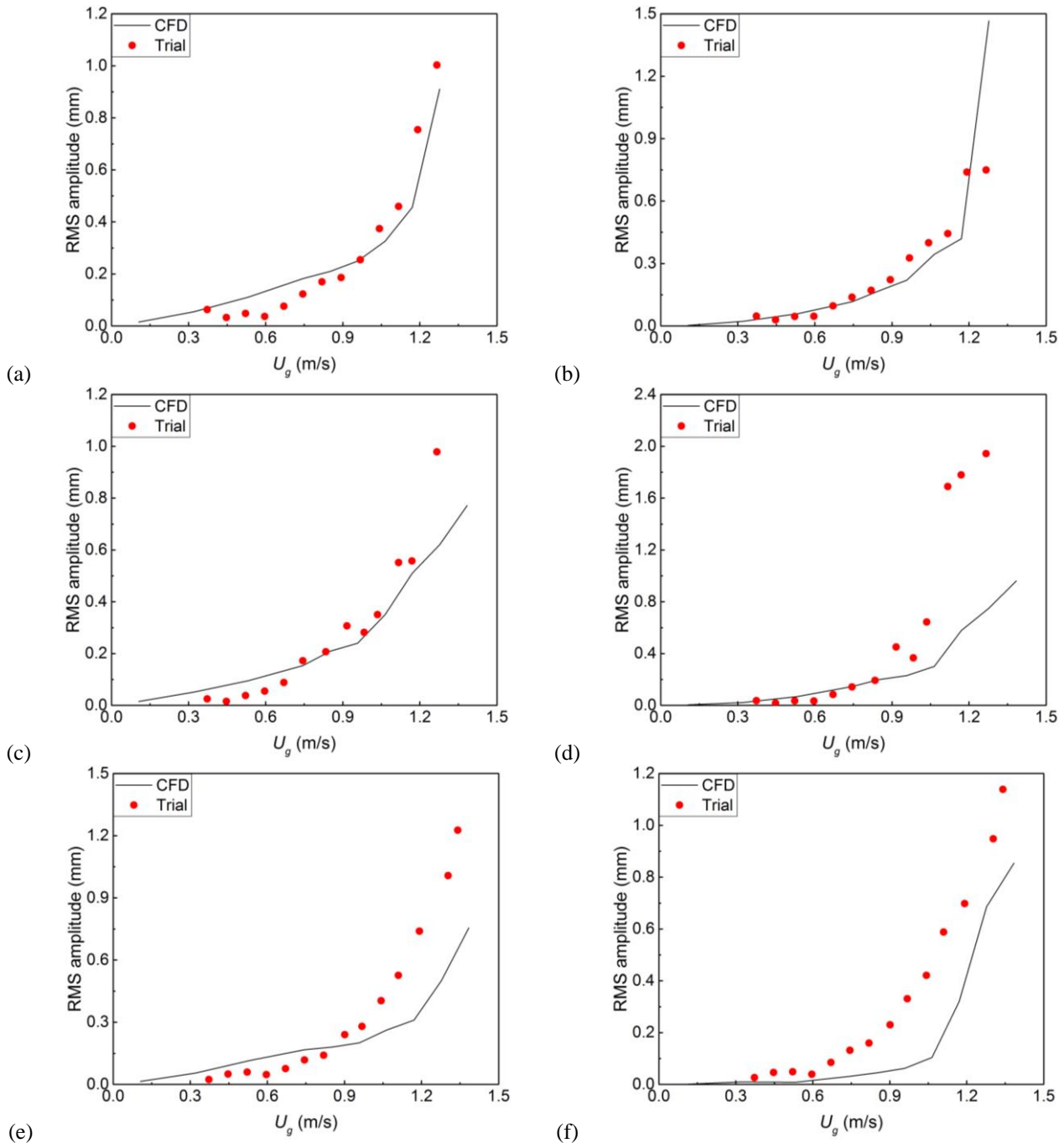


Fig. 10 Curve of RMS amplitude to mean gap velocity. (a) 0-degree angle, stream-wise; (b) 0-degree angle, cross-stream; (c) 15-degree angle, stream-wise; (d) 15-degree angle, cross-stream; (e) 30-degree angle, stream-wise; (f) 30-degree angle, cross-stream

Table 3 Critical flow velocity obtained by trial and CFD methods

Tube arrangement	Vibration direction	Trial method /(m/s)	CFD method /(m/s)	Relative error /%
0-degree angle	stream-wise	1.12	1.17	4.5
	cross-stream	1.12	1.17	4.5
15-degree angle	stream-wise	1.04	1.17	12.5
	cross-stream	0.98	1.06	8.3
30-degree angle	stream-wise	1.04	1.17	12.5
	cross-stream	1.04	1.06	1.9

According to the results in Table 3, 0-degree angle arrangement is least likely to be unstable and the instability occurs firstly in 15-degree angle arrangement in the cross-stream direction.

The experimental results are compared with former researches summarized by Au-Yang [28], shown in Fig. 11. The data points in this paper are all above the suggested line around the mean line. Therefore, it can be considered that the existing experience coefficient  $K$  still applies to the concentric arrays in this paper. It can also be seen from Fig. 11 that the 0-degree angle arrangement is the most stable and the 15-degree angle arrangement is the most unstable.

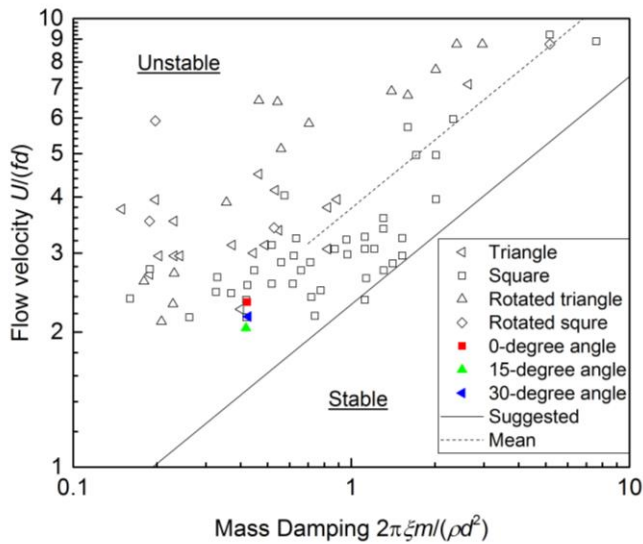


Fig. 11 Stability diagram for tube arrays

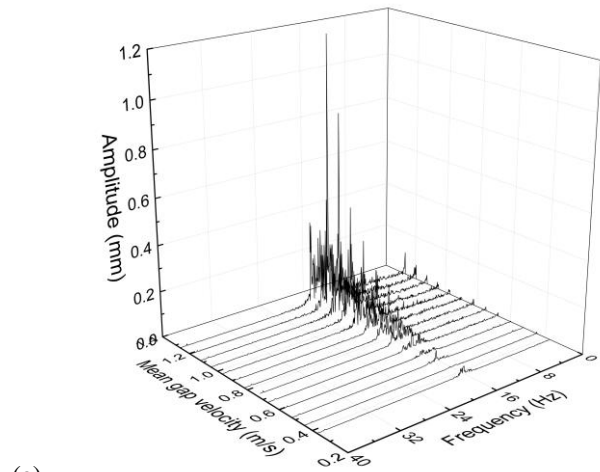
### Spectral response

Spectral response of tubes reflects the coupling frequency of interaction between the tube bundle and surrounding flow field. The change of spectrum from a wide band to a narrow band indicates the occurrence of FEI, where the narrower the band is after instability, the stronger the instability of the tube bundle is. In general, the vibration of the tube in the cross-stream direction is considered more [29]. Accordingly, the spectral response of cross-stream direction is mainly discussed.

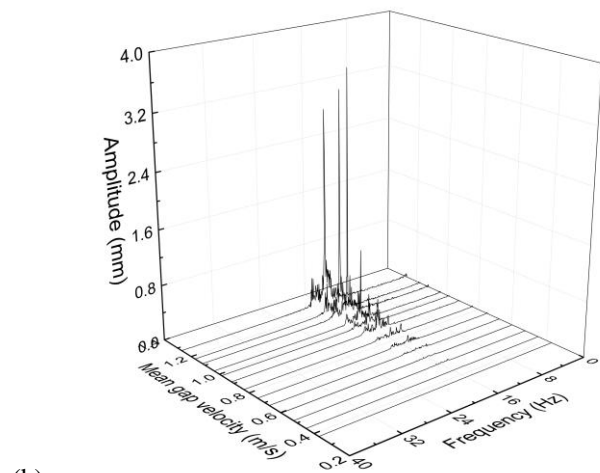
Spectral response of tubes at different locations are shown in Fig. 12. At low flow velocities, turbulence buffeting occurred mainly in the tube bundle in a wider band at different coupling frequencies, and as the flow rate increasing, it converted to a narrow band at a single frequency, which was called main vibration frequency. Critical flow velocity could also be estimated from the spectral response [11, 30].

It was noted that at the 15-degree angle, the response amplitude of the tube at the main vibration frequency was in a declining trend after instability, which might be affected by the “static drag effect”. The 0-degree angle and the 30-degree angle were symmetric, while the 15-degree angle was asymmetric. Therefore, at 15-degree angle, a drag force that was biased to one side was generated in the cross-stream

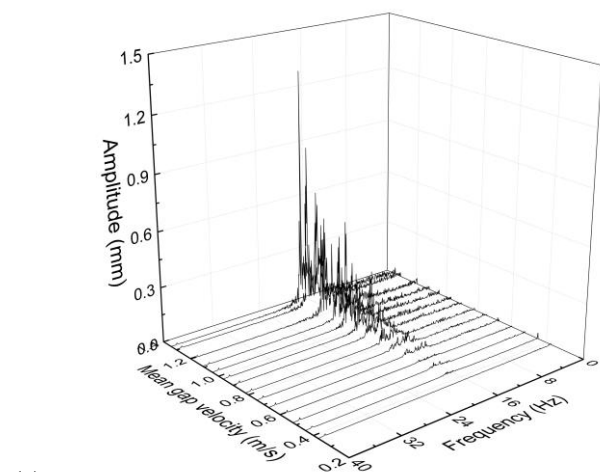
direction. Due to the drag force, the tube bundle deviated from original equilibrium position, resulting in a change in the tube bundle formation, which affected the vibration of the tube bundle.



(a)



(b)



(c)

Fig. 12 Spectral response of tubes at different locations. (a) 0-degree angle; (b) 15-degree angle; (c) 30-degree angle



## Main vibration direction

The main vibration direction can be achieved through the observation of the tracks of the tube bundles. It will further deepen the understanding of the instability behavior of the tube bundle. The tracks of the tube bundles were obtained by simulation method, shown as Fig. 13. When the gap velocity was small, the amplitudes of tube bundles in the stream-wise direction was larger. As the gap velocity increasing, the amplitudes of the tube bundles in the cross-stream direction were larger and approximate periodic motion was formed when

vibrations were completely controlled by FEI. This change of vibrational mode has also been mentioned in a previous study by Chen [11].

Moreover, front tubes showed more displacement than rear tubes in Fig. 13. This was mainly due to the fact that tubes in the front row was directly in contact with the external turbulence, subjected to a greater impact and absorbed more energy, while the rear row tubes were less affected. Still, the displacement of rear tubes was not negligible, that would have a greater impact on the equipment.

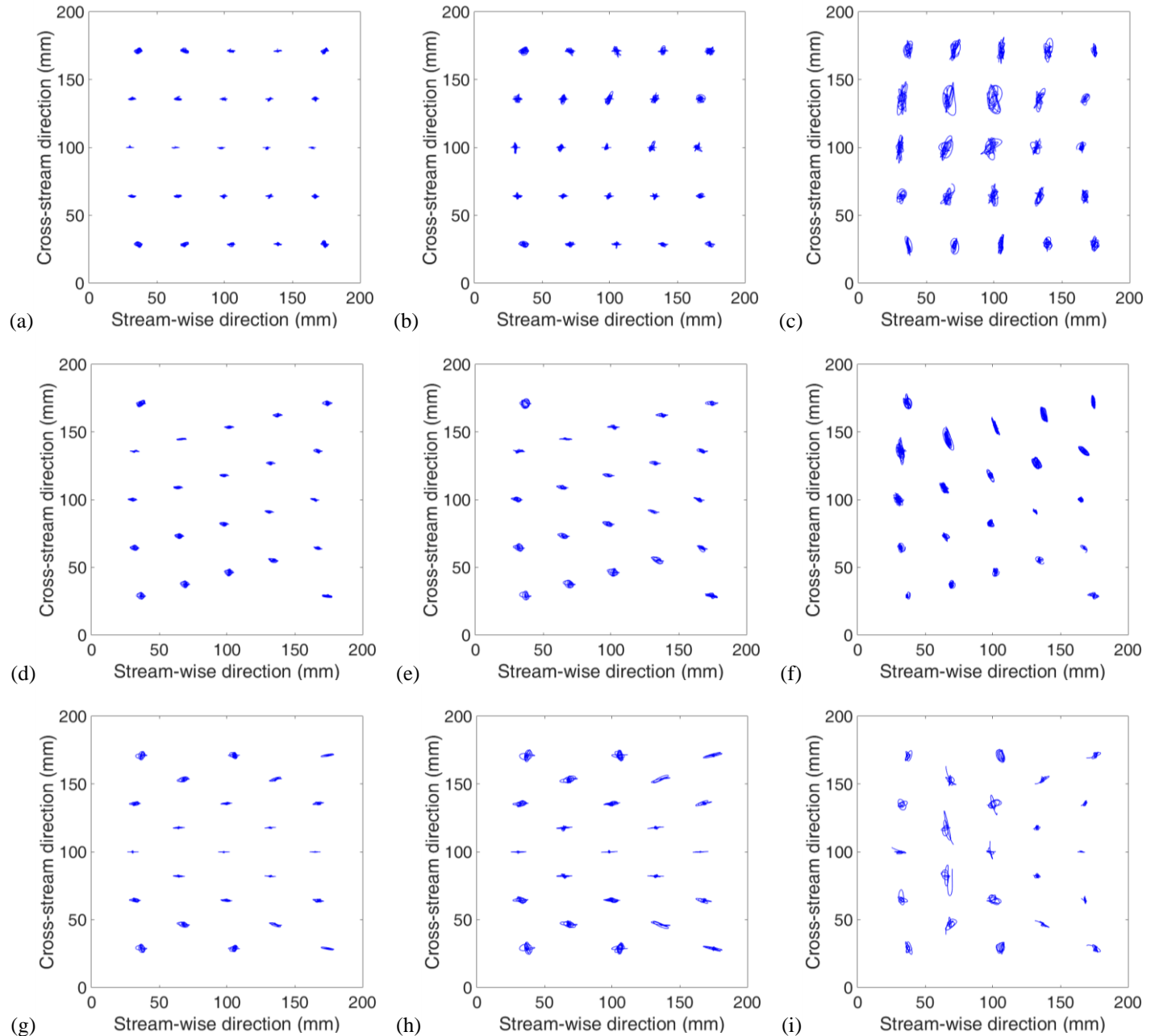


Fig. 13 Tracks of the tube bundles (scale: 2). (a) 0-degree angle,  $U_g = 1.06$  m/s; (b) 0-degree angle,  $U_g = 1.17$  m/s; (c) 0-degree angle,  $U_g = 1.28$  m/s; (d) 15-degree angle,  $U_g = 1.17$  m/s; (e) 15-degree angle,  $U_g = 1.28$  m/s; (f) 15-degree angle,  $U_g = 1.38$  m/s; (g) 30-degree angle,  $U_g = 1.17$  m/s; (h) 30-degree angle,  $U_g = 1.28$  m/s; (i) 30-degree angle,  $U_g = 1.38$  m/s

## CONCLUSION

In this paper, the FEI of concentric arrays of tube bundles subjected on cross flow is studied. A water tunnel experimental device based on visual image processing system is set up and ANSYS CFX is adopted for numerical simulation. Critical flow velocity, main vibration direction, vibration frequency and other characteristics are studied. The tube bundles at the three selected locations are analyzed comparatively. The main conclusions of this paper are as follows.

(1) Through the free attenuation vibration test, it can be concluded that the results of visual vibration measurement method and traditional strain test method are in good agreement, and the visual vibration test method has the advantages of simple installation and small influence on the flow field.

(2) The critical flow velocity can be obtained from RMS amplitudes at different flow velocities. The 15-degree angle arrangement is the most instable location, and the instability occurs firstly in the cross-stream direction.

(3) By analyzing the amplitudes of the main vibration frequency in the spectral responses, it can be seen that the static drag effect occurs at the 15-degree angle arrangement, while does not appear at 0-degree angle and 30-degree angle arrangement. Compared with the other two arrangements, there is no symmetry at 15-degree angle arrangement, resulting in the drag force that is biased to one side in the cross-stream direction. The tube bundle deviates from the original equilibrium position and the vibration is affected.

(4) By analyzing the vibration track diagrams, it can be concluded that with the increase of flow velocity, the tube vibration firstly occurs in the stream-wise direction and then in the cross-stream direction. The amplitudes of the front tubes are greater than that of the rear tubes. Therefore, the outermost tubes at the entrance should be paid more attention to in engineering practice.

## ACKNOWLEDGMENTS

This work was supported by a grant from Lanpec Technologies Limited of China National Machinery Industry Corporation.

## REFERENCES

- [1] Pettigrew, M. J., Sylvestre Y., and Campagna A. O., 1978, "Vibration analysis of heat exchanger and steam generator designs," *Nuclear Engineering and Design*, 48(1), pp. 97-115. DOI: 10.1016/0029-5493(78)90211-X
- [2] Gorman, D. J., 1979, "An overview of the subject of liquid cross-flow induced vibration of heat exchanger tube bundles," *Vibration in nuclear plant. Proceedings of international conference held at Keswick, UK in May 1978.*
- [3] Weaver, D. S., Ziada, S., Au-Yang, M. K., et al, 2000, "Flow-induced vibrations in power and process plant components—progress and prospects," *Journal of Pressure Vessel Technology*, 122(3), pp. 339-348. DOI: 10.1115/1.556190
- [4] Chen, S. S., 1987, "A general theory for dynamic instability of tube arrays in crossflow," *Journal of Fluids and Structures*, 1(1), pp. 35-53. DOI: 10.1016/S0889-9746(87)90170-8
- [5] Connors, H. J., 1970, "Fluidelastic vibration of tube arrays excited by cross flow," *Proc. ASME Winter Annual Meet.*, 1970.
- [6] Blevins, Robert D., 1990, "Flow-induced vibration."
- [7] Price, S. J., and M. P. Paidoussis, 1984, "An improved mathematical model for the stability of cylinder rows subject to cross-flow," *Journal of Sound and Vibration*, 97(4), pp. 615-640. DOI: 10.1016/0022-460X(84)90512-1
- [8] Granger, S., and M. P. Paidoussis, 1996, "An improvement to the quasi-steady model with application to cross-flow-induced vibration of tube arrays," *Journal of Fluid Mechanics*, 320, pp. 163-184. DOI: 10.1017/S0022112096007495
- [9] Tanaka, H., and S. Takahara, 1981, "Fluid elastic vibration of tube array in cross flow," *Journal of sound and vibration*, 77(1), pp. 19-37. DOI: 10.1016/S0022-460X(81)80005-3
- [10] Lever, J. H., and D. S. Weaver, 1986, "On the stability of heat exchanger tube bundles, part 1: Modified theoretical model," *Journal of Sound and vibration*, 107(3), pp. 375-392. DOI: 10.1016/S0022-460X(86)80114-6
- [11] Chen, Shoei-Sheng, 1987, "Flow-induced vibration of circular cylindrical structures."
- [12] Roberts, Benjamin Washington, 1962, "Low frequency, self-excited vibration in a row of circular cylinders mounted in an airstream," *Diss. University of Cambridge, Eng.*
- [13] Lever, J. H., and D. S. Weaver, 1986, "On the stability of heat exchanger tube bundles, part 2: Numerical Results and Comparison with Experiments," *Journal of Sound and vibration*, 107(3), pp. 393-410.
- [14] Grover, L. K., and D. S. Weaver, 1978, "Cross-flow induced vibrations in a tube bank—vortex shedding," *Journal of Sound and Vibration*, 59(2), pp. 263-276. DOI: 10.1016/0022-460X(78)90505-9
- [15] Pttigrew, M. J., Taylor C. E., Jong J. H., et al, 1995, "Vibration of a tube bundle in two-phase freon cross-flow," *Journal of Pressure Vessel Technology*, 117(4), pp. 321-329. DOI: 10.1115/1.2842130
- [16] Prakash, V., Thirumalai, M., Prabhakar, R., et al, 2009, "Assessment of flow induced vibration in a sodium-sodium heat exchanger," *Nuclear Engineering and Design*, 239(1), pp. 169-179. DOI: 10.1016/j.nucengdes.2008.10.007
- [17] Chen, S. S., Cai Y., and Zhu S., 1996, "Flow-Induced Vibration of Tubes in Cross-Flow," *Journal of Offshore Mechanics and Arctic Engineering*, 118(4), pp. 253-258. DOI: 10.1115/1.2833913
- [18] Huňady, Róbert, and Martin Hagara, 2017, "A new

- procedure of modal parameter estimation for high-speed digital image correlation,” *Mechanical Systems and Signal Processing*, 93, pp. 66-79. DOI: 10.1016/j.ymsp.2017.02.010
- [19] Chu, T. C., Ranson W. F., and Sutton M. A., 1985, “Applications of digital-image-correlation techniques to experimental mechanics,” *Experimental mechanics*, 25(3), pp. 232-244. DOI: 10.1007/BF02325092
- [20] Sutton M. A., Wolters W. J., Peters W. H., et al, 1983, “Determination of displacements using an improved digital correlation method,” *Image and vision computing*, 1(3), pp. 133-139. DOI: 10.1016/0262-8856(83)90064-1
- [21] Hagara, Martin, Róbert Huňady, and František Trebuňa, 2015, “Stress Analysis Performed in the Near Surrounding of Small Hole by a Digital Image Correlation Method,” *Acta Mechanica Slovaca*, 18(3-4), pp. 74-81. DOI: 10.1515/mopa-2014-0033
- [22] Sutton, Michael A., Jean Jose Orteu, and Hubert Schreier, 2009, “Image correlation for shape, motion and deformation measurements: basic concepts, theory and applications,” Springer Science & Business Media.
- [23] Hassan, Yassin A., and Ibrahim Wael A., 1997, “Turbulence prediction in two-dimensional bundle flows using large-eddy simulation,” *Nuclear technology*, 119(1), pp. 11-28. DOI: 10.13182/NT77-A35391
- [24] Barsamian, H. R., and Hassan Y. A., 1997, “Large eddy simulation of turbulent crossflow in tube bundles,” *Nuclear Engineering and Design*, 172(1-2), pp. 103-122. DOI: 10.1016/S0029-5493(97)00034-4
- [25] Bouris, D., and Bergeles G., 1999, “Two dimensional time dependent simulation of the subcritical flow in a staggered tube bundle using a subgrid scale model,” *International journal of heat and fluid flow*, 20(2), pp. 105-114. DOI: 10.1016/S0142-727X(98)10053-X
- [26] Hassan, Yassin A., and Barsamian Hagop R., 1999, “Turbulence simulation in tube bundle geometries using the dynamic subgrid-scale model,” *Nuclear technology*, 128(1), pp. 58-74. DOI: 10.13182/NT99-A3014
- [27] Omar, Hossin, 2012, “Numerical Simulations of Fluidelastic Instability in Tube Bundles,” University of New Brunswick (Canada).
- [28] Au-Yang, M. K., R. D. Blevins, and T. M. Mulcahy, 1991, “Flow-Induced Vibration Analysis of Tube Bundles—A Proposed Section III Appendix N Nonmandatory Code,” *Journal of Pressure Vessel Technology*, 113(2), pp. 257-267. DOI:10.1115/1.2928753
- [29] Khalifa, Ahmed, David Weaver, and Samir Ziada, 2012, “A single flexible tube in a rigid array as a model for fluidelastic instability in tube bundles,” *Journal of Fluids and Structures*, 34, pp. 14-32. DOI: 10.1016/j.jfluidstructs.2012.06.007
- [30] Mureithi, N. W., Zhang C., Ruel M., et al, 2005, “Fluidelastic instability tests on an array of tubes preferentially flexible in the flow direction,” *Journal of fluids and structures*, 21(1), pp. 75-87. DOI: